Therapeutics, Targets, and Chemical Biology

Cancer Research

Modulation of the ATPase and Transport Activities of Broad-Acting Multidrug Resistance Factor ABCC10 (MRP7)

Ekaterina V. Malofeeva, Natalya Domanitskaya, Mariya Gudima, and Elizabeth A. Hopper-Borge

Abstract

The cell surface molecule ABCC10 is a broad-acting transporter of xenobiotics, including cancer drugs, such as taxanes, epothilone B, and modulators of the estrogen pathway. *Abcc10*$^{-/-}$ mice exhibit increased tissue sensitivity and lethality resulting from paclitaxel exposure compared with wild-type counterparts, arguing ABCC10 functions as a major determinant of taxane sensitivity in mice. To better understand the mechanistic basis of ABCC10 action, we characterized the biochemical and vectorial transport properties of this protein. Using crude membranes in an ABCC10 overexpression system, we found that the ABCC10 transport substrates estrogen estradiol-glucuronide ($E_2$17βG) and leukotriene C4 (LTC_4) significantly stimulated ABCC10 beryllium fluoride (BeFx)-sensitive ATPase activity. We also defined the $E_2$17βG antagonist, tamoxifen, as a novel substrate and stimulator of ABCC10. In addition, a number of cytotoxic substrates, including docetaxel, paclitaxel, and Ara-C, increased the ABCC10 basal ATPase activity. We determined that ABCC10 localizes to the basolateral cell surface, using transepithelial well assays to establish that ABCC10-overexpressing LLC-PK1 cells exported [^{3}H]-docetaxel from the apical to the basolateral side. Importantly, we found that the clinically valuable multikinase inhibitor sorafenib, and a natural alkaloid, cepharanthine, inhibited ABCC10 docetaxel transport activity. Thus, concomitant use of these agents might restore the intracellular accumulation and potency of ABCC10-exported cytotoxic drugs, such as paclitaxel. Overall, our work could seed future efforts to identify inhibitors and other physiologic substrates of ABCC10. *Cancer Res; 72(24); 6457–67. ©2012 AACR.*

Introduction

The phenomenon of multidrug resistance (MDR) remains a substantial problem in the chemotherapeutic treatment of cancer. One important contributing factor in MDR is the overexpression of a class of efflux pumps known as ATP-binding cassette (ABC) transporters. The C subfamily of ABC proteins is alternatively known as the ABCC proteins, or the multidrug resistance protein (MRP) subfamily. Members of this subfamily confer resistance to and transport several classes of chemotherapeutics including taxanes, vinca alkaloids, camptothecans, and nucleoside analogs, as well as physiologic substrates including leukotrienes and glutathione (1, 2). This ABCC group consists of 9 family members conserving a common structural organization that includes at least 2 transmembrane domains (TMD) and nucleotide-binding domains (NBD; ref. 2). The ABCC subfamily is further divided into 2 groups: ABCC1 (MRP1), ABCC2 (MRP2), ABCC3 (MRP3), ABCC6 (MRP6), and ABCC10 (MRP7) have additional N-terminal transmembrane domains, whereas ABCC4 (MRP4), ABCC5 (MRP5), ABCC11 (MRP8), and ABCC12 (MRP9) do not (2).

ABCC10 consists of 3 TMDs and 2 NBDs, and is one of the least well-characterized family members (3), although we and others have shown that ABCC10 tissue expression is widespread (4). Recent work has suggested that ABCC10 expression level is elevated in non–small cell lung cancer (NSCLC) in relation to normal lung, with ABCC10 expression in adenocarcinoma correlated with tumor grade and stage (5). Supporting a potential role for ABCC10 in control of the response of tumors to the administration of therapeutics, we have previously shown that overexpression of ABCC10 *in vitro* confers resistance to an unusually wide range of clinically valuable drugs, including taxanes, vinca alkaloids, nucleoside analogs, and epothilone B (6–8). Excitingly, we have recently used a newly developed Abcc10$^{-/-}$ mouse model to show that absence of this transporter *in vivo* sensitizes animals to taxanes, with Abcc10$^{-/-}$ mice experiencing increased sensitivity (i.e., neutropenia, and bone marrow hypoplasia) as compared with their wild-type counterparts following paclitaxel treatment.

Together, these findings suggest that modulation of ABCC10 activity by inhibitors may have clinical value in management of human cancers, such as NSCLC. Currently ATPase activities have been described for some of the longer ABCC subfamily members, including ABCC1, ABCC2, ABCC3, and ABCC6

Authors' Affiliation: Program in Developmental Therapeutics, Fox Chase Cancer Center, Philadelphia, Pennsylvania

Note: Supplementary data for this article are available at Cancer Research Online (http://cancerres.aacrjournals.org/).

Corresponding Author: Elizabeth Hopper-Borge, Fox Chase Cancer Center, 333 Cottman Avenue, Philadelphia, PA 19111. Phone: 215-214-1505; Fax: 215-728-3616; E-mail: EA_Hopper@fccc.edu

doi: 10.1158/0008-5472.CAN-12-1340

(9–12) and also for ABCC4 (13). However, to date, neither the enzymatic activity of the ABCC10 ATPase nor the mechanistic basis for ABCC10 transport of substrates have been substantially investigated. This study addresses these points, by characterizing the effects of modulators on biochemical and transport properties of ABCC10.

Materials and Methods

Cell lines

LLC-PK1 cells were purchased from the American Type Culture Collection (ATCC) 7 years ago. All ATCC cell lines undergo authentication tests during the accessioning process using methods described in the online ATCC brochure *Maintaining High Standards in Cell Culture*. These characterizations are applied to the final seed and distribution stocks of cell lines for certification include testing viability of the cell population just before freezing and immediately after thawing by Trypan-blue dye exclusion test. Observations of recovery and growth are recorded along with morphologic appearance. The ATCC also uses isoenzymology and/or the cytochrome C subunit I (COI) PCR assay is conducted for species confirmation. Cells were passaged in our laboratory for fewer than 3 months after receipt or resuscitation. The High Five cell line was purchased 3 years ago from Invitrogen. Cells were passaged in our laboratory for fewer than 3 months after receipt or resuscitation. These cells have not been authenticated.

Reagents

Trizma hydrochloride, D-mannitol, EGTA, dithiothreitol, ammonium molybdate, antimony potassium tartarate, sulfuric acid, potassium chloride, ouabain powder, magnesium chloride, L-ascorbic acid, SDS, sodium azide, beryllium sulfate tetrahydrate, sodium fluoride, sodium orthovanadate (Vi), cobalt (II) chloride, calcium chloride, manganese (II) chloride, protease inhibitors, bovine serum albumin (BSA), glycerol, ATP, ADP, lucifer yellow CH dipotassium salt, tamoxifen, 17β-estradiol-D-17β-glucuronide, glutathione, leukotriene C4 (LTC_4), docetaxel, paclitaxel, cytosine β-D-arabinofuranoside (Ara-C), cisplatinum, and epothilone B were purchased from Sigma-Aldrich. [^{3}H]-docetaxel (5 Ci/mmol) was obtained from Moravek Biochemicals Inc.

Preparation of ABCC10-transfected LLC-PK1 cells

ABCC10 expression vector and parental plasmid were transfected into LLC-PKI cells using Lipofectamine (according to the manufacturer's instructions, Invitrogen). Individual colonies were selected in medium containing gentamicin (1,000 μg/mL) and expanded for further analysis. Two clones in which ABCC10 protein was detected by immunoblot analysis were used in the present study. The cells are routinely tested (every 3–6 months) for mycoplasma contamination and for ABCC10 protein expression. LLC-ABCC10 and empty vector–transfected control cells were cultured in medium 199 supplemented with 10% FBS, 50 U/mL penicillin, 50 μg/mL streptomycin, 2 mmol/L L-glutamine, and 800 μg/mL gentamicin. All cell lines were grown at 37°C with 5% CO_2 under humidifying conditions.

Expression and identification of ABCC10, ABCB1 and ABCC1 in High Five insect cells

High Five insect cells (Invitrogen) were infected with the recombinant baculovirus containing the ABCB1 (Addgene plasmid 10957), ABCC1 or ABCC10 cDNA. To create the recombinant baculovirus, ABCB1, ABCC1 and ABCC10 cDNA were cloned into pFastBac CT-TOPO vector (Invitrogen). Crude membranes were prepared as previously described (14) and used in subsequent ATPase assays. Total protein was estimated using an Amido Black protein-filter assay of Schaffner and Weissmann with BSA as a standard. The membrane fraction was then resuspended to a concentration of 1 mg/mL and stored at −80°C until use. Crude membranes were electrophoresed on a 3% to 8% NuPAGE gel (Invitrogen) and stained with Colloidal blue (Invitrogen) following the manufacturer's instructions. Following electrotransfer to nitrocellulose paper, blots were probed with the previously described ABCC10 monoclonal antibody at a dilution of 1:10 (7) or the previously described Abcc10 polyclonal antibody (15) at a dilution of 1:3,000 and an anti-ABCC1 mouse monoclonal QCRL-1 (Santa Cruz Biotechnology, Inc.) at a dilution of 1:100.

Preparation of membranes

Total cell membranes were prepared from LLC-PK1 cells by Dounce homogenization in Plasma Membrane (PM) PM-buffer (1 mol/L HEPES, 1 mol/L $MgCl_2$, and 1 mol/L KCl) containing protease inhibitors: 5 μg/mL aprotinin, 5 μg/mL leupeptin, 2 μg/mL pepstatin, 100 mmol/L phenylmethylsulfonylfluoride (PMSF). Intact cells and nuclei were removed by centrifugation at 500 × *g* for 10 minutes at 4°C, and then the supernatant spun at 3,000 × *g* for 10 minutes at 4°C. Cell membranes were pelleted by centrifugation at 10,000 × *g* for 45 minutes at 4°C and resuspended in PM-buffer.

For immunoblot analysis, 10 to 40 μg of membrane proteins was analyzed on a 8% SDS-PAGE gel and transferred to nitrocellulose filters using a wet transfer system, as described previously (16). The blots were incubated with the previously described ABCC10 monoclonal antibody at a dilution of 1:10 (7) or the previously described Abcc10 polyclonal antibody (15). After washing, the blots were incubated with horseradish peroxidase (HRP) secondary goat anti-rabbit immunoglobulin G (IgG; NEN). β-Actin-HRP (Abcam) conjugated antibody was used at a dilution of 1:5,000.

Beryllium fluoride-induced [α-^{32}P]-8-azidoADP trapping in ABCC10

Beryllium fluoride (BeFx)-induced [α-^{32}P]-8-azidoADP trapping assays contained ATPase assay buffer, 0.5 mmol/L BeFx, 20 mmol/L $MgCl_2$, 1 mg/mL of membrane ABCC10, and 100 μmol/L [α-^{32}P]-8-azidoATP (2.5–10 μCi/nmol; Affinity Photoprobes, LLC). Reactions were preincubated in low light in the absence of [α-^{32}P]-8-azidoATP at 37°C for 3 minutes, initiated by the addition of [α-^{32}P]-8-azidoATP and quenched by adding ice-cold ATP (100 mmol/L). Reactions were irradiated by UV light (365 nm wavelength) on ice for 10 minutes and subjected to SDS-PAGE, and after drying, the gel was exposed to film for 12 to 72 hours.

Measurement of ATPase activity

ATPase activity was measured by the endpoint inorganic phosphate (Pi) assay as previously described (17). ABCC10-, ABCB1- and ABCC1-specific activity was recorded as vanadate- or BeFx-sensitive ATPase activity. The amount of inorganic phosphate released over 20 minutes at 37°C was measured. 2× ATPase assay buffer (100 mmol/L Tris–HCl pH 7.5, 1 mol/L KCl, 0.25 mol/L sodium azide, 0.125 mol/L EGTA, 1 mmol/L ouabain, and 1 mol/L dithiothreitol (DTT)) was combined with 2 mol/L $MgCl_2$, 5 to 10 μg of membrane protein, and various drugs or substrates for a 5-minute preincubation at 37°C. The reaction was initiated by 5 mmol/L ATP addition and quenched with 100 μL of 5% SDS. The amount of Pi released was quantitated using a previously described colorimetric method (13). Kinetic parameters were determined by linear regression analysis of the Lineweaver–Burk transformation of the data by using GraphPad Prism 4 software. Velocity (V) = V_{max} [S]/([S] + K_m), in which: V_{max} is the limiting velocity as substrate concentrations get very large. [S] is concentration of substrate; K_m is the concentration of substrate that leads to half-maximal velocity (in mol/L). All data were statistically analyzed with a Student unpaired t test, and P values less than 0.05 were considered statistically significant.

Drug accumulation

For drug accumulation, control LLC-pcDNA 3.1 cells, ABCC10-transfected LLC-ABCC10-11, and LLC-ABCC10-16 cells were seeded in duplicate at a density of 2×10^5 cells per well in a 6-well plate. The next day, the media was replaced with media containing 0.1 μmol/L [^{3}H]-docetaxel (5 Ci/mmol, Movarek) to a final concentration and cells were incubated at 37°C. For inhibition studies, the cells were preincubated with the modulators cepharanthine (5 μmol/L) or tyrosine kinase inhibitors (TKI) as indicated in the results (2.5 μmol/L) for 1 hour. After preincubation, the solution was removed and labeled substrate with modulators was added to the well for 15, 30, and 60 minutes incubation at 37°C. After incubation, cells were washed with ice-cold PBS and trypsinized. An aliquot of cells was used to determine cell number, and the remaining cells were then washed 3 times with ice-cold PBS. Each sample was placed in scintillation fluid to measure the radioactivity in a liquid scintillation counter. All data were statistically analyzed with a Student unpaired t test, and P values less than 0.05 were considered statistically significant.

Transepithelial transport

Cells were seeded on microporous polycarbonate membrane filters (3.0-μm pore size, 6.5-mm insert, Transwell 3415, Costar) at a density of 1×10^6 cells per well for LLC-PK1 cells in 24-well plates. The cells were grown for 7 days in complete medium, with medium replacement after day 1 and then every 2 days until the day of the experiment. Once the transepithelial electrical resistance (TEER) reached more than 500 Ωcm^2 and when Lucifer yellow rejection reached 97% to 100% (18, 19), the experiment was started by adding Hank's Balanced Salt Solution(HBSS)-containing 0.1 μmol/L [^{3}H]-docetaxel (5 Ci/mmol) to either the apical or basolateral side. For the inhibition study, after washing steps, the cells were preincubated with modulators for 1 hour. After incubation, the solutions were aspirated and labeled substrate was added to the donor chamber, while refilling fresh modulator solution in both chambers. The cells were incubated at 37°C in 5% CO_2, and 25 μL aliquots were taken from the receiver side at 0, 2, 6, 12, 20, and 30 minutes, and placed in scintillation fluid to measure the radioactivity in liquid scintillation counter. The apparent permeability coefficient (P_{app}) was calculated as previously described (19). All data were statistically analyzed with a Student unpaired t test, and P values less than 0.05 were considered statistically significant.

Confocal laser scanning microscopy

LLC-PK ABCC10 transfectants were grown on cover slips for approximately 3 days until cells reached confluency. After PBS washing, fixation, solubilization, and blocking, cells were incubated with rabbit polyclonal C-terminus-ABCC10 antibody (diluted 1:50 in blocking buffer; ref. 15) and mouse anti-β-catenin (dilution 1:500; BD Transduction Laboratories) for 1 hour at room temperature. Secondary antibody included anti-rabbit conjugated to Alexa-488 and anti-mouse conjugated to Alexa-568. 4′,6-Diamidino-2-phenylindole (DAPI; Molecular Probes/Invitrogen) was used to stain DNA at a dilution of 1:2,000. The cells were mounted on a glass slide with ProLonged Antifade Reagent (Molecular probes). Confocal laser scanning microscopy was conducted with a Nikon C1 spectral confocal microscope (Nikon).

Results

Expression and identification of human ABCC10 and ABCC1 in High Five insect cells

To support study of ABCC10 ATPase activity, ABCC10 and ABCC1 (a well-characterized transporter used as a positive control; refs. 20, 21) were overexpressed using a baculovirus system. ABCC10 and ABCC1 were readily detected in crude membrane fractions as full-length proteins, with almost no truncation or degradation byproducts (Fig. 1A and B). Purified ABCC10 bound effectively to the nucleotide analog [α-^{32}P]-8-azidoATP, confirming structural integrity of the NBDs (13; Fig. 1C).

Basal properties of ABCC10-mediated ATP hydrolysis

ABCC10 ATPase activity was measured using an Pi release assay (17), with ouabain, EGTA, and sodium azide added to crude membrane preparations to eliminate confounding Na^+/K^+, Ca^{2+} and mitochondrial ATPase activity, as in ref. (22). Under these conditions, the basal rate of ATP hydrolysis of ABCC10 ranged from 5.5 to 12 nmol/min/mg protein (Fig. 2A and data not shown), depending on the preparation. For reference, ABCC1 activity was 5 to 10 nmol/min/mg protein using purified and reconstituted protein (9), and approximately 4 to 5 nmol/min/mg protein in our system (data not shown). The noncovalent ATPase inhibitors Vi and BeFx replace phosphate during ATP hydrolysis, and stabilize a specific, transition state conformation, inhibiting ATPase activity; prior work has shown individual ABC transporters respond differently to these inhibitors, reflecting differences in catalytic activity (13, 23, 24). We determined that ABCC10 ATPase activity is

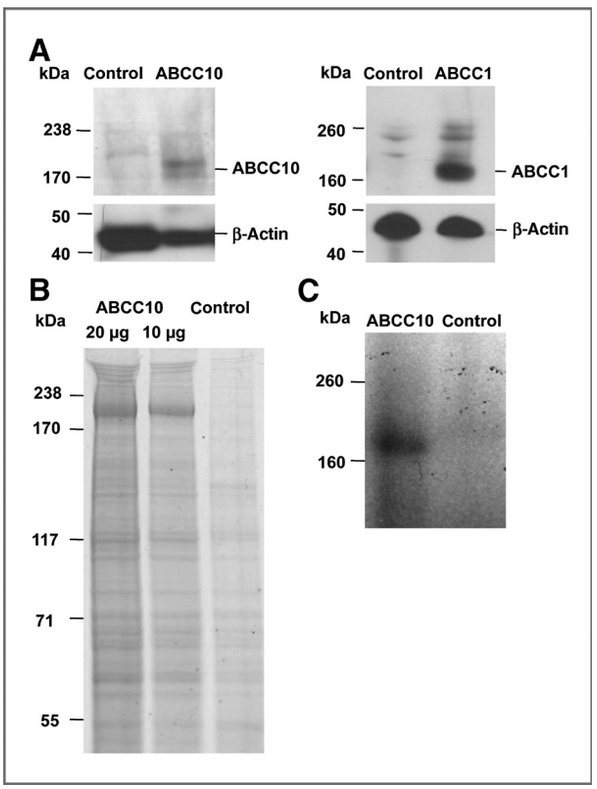

Figure 1. Detection of ABCC10 and ABCC1 in membrane vesicle preparation. A, membrane vesicles prepared from High Five insect cells infected with ABCC10, ABCC1, or control baculovirus were resolved by SDS-PAGE and probed with anti-ABCC10 or anti-ABCC1 antibodies. Full length ABCC10 is approximately 191 kDa, and ABCC1 is approximately 170 kDa (6, 17). B, colloidal blue staining of (i) 20 μg or (ii) 10 μg of membrane preparation indicates no degradation. C, autoradiograph indicating binding of [α-^{32}P]-8-azido ATP to ABCC10, after incubation of High Five ABCC10 overexpressed membranes with [α-^{32}P] 8-azidoATP under a nonhydrolytic condition (4°C).

more sensitive to BeFx than Vi (32% and 11.4% inhibition, respectively; Fig. 2A and B). For ABCC1, the BeFx-dependent inhibition was almost 2-fold more effective than Vi inhibition (60% vs. 35%, respectively), in accordance with previously reported values (25; Fig. 2A and B).

Environmental pH can significantly affect transporter ATPase activity (19, 22, 26–28). Optimal ABCC10 ATPase activity occurred at pH 7.5 (Fig. 2C), comparable with that reported for ABCC1 (9). Titration of ATP revealed maximal ABCC10 activity at a concentration of approximately 6 mmol/L (Fig. 2D). We analyzed the kinetics over a concentration range from 0 to 8 mmol/L ATP using a Lineweaver–Burk analysis. We determined that the ABCC10 K_m value for ATP binding is 3.2 mmol/L, in contrast to a 0.1 mmol/L K_m value of ABCC1 (25). ABCC10 ATPase activity was inhibited at [ATP] more than 9 mmol/L. Prior work on other ATPases have observed similar inhibitory effects under conditions where other factors required for catalysis, such as [Mg^{2+}], are present in limiting concentrations (29). Discrete ATPases typically have varying requirements for divalent cations during ATP hydrolysis (13, 30). As anticipated, ABCC10-mediated ATP hydrolysis is cation dependent; we established a rank order preference of Mn^{2+}>Mg^{2+}>Ca^{2+}>Co^{2+} (Fig. 2E), with Mn^{2+} increasing ATPase activity by 52% as compared with Mg^{2+}.

Dose-dependent induction of ABCC10 ATPase activity by physiologic substrates and anticancer agents

LTC_4, the estrogen estradiol-glucuronide ($E_2$17βG) and glutathione are physiologic substrates for ABCC1, and induce ABCC1 ATPase activity (31, 32). We tested these compounds for activation of ABCC10, using the crude membrane system described earlier. We found that LTC_4 and $E_2$17βG induced ABCC10 ATPase activity by 79.7% and 30%, respectively (Fig. 3A and C). Maximal induction of ABCC10 ATPase activity was observed for LTC_4 at 1 μmol/L. Further analyses of the effect of LTC_4 on ABCC10 ATPase activity revealed that at concentrations less than 1 μmol/L, the $K_m = 0.057$ μmol/L for LTC_4 (Fig. 3C inset). The compound tamoxifen is frequently used in breast cancer treatments as an estrogen receptor antagonist, based on competition with estradiol. Interestingly, we found that tamoxifen is also a modest substrate for ABCC10, and at lower tamoxifen concentrations (less than 2 μmol/L) the $K_m = 0.078$ μmol/L (Fig. 3B inset). However, at higher concentrations LTC_4 and tamoxifen both inhibited ABCC10 ATPase activity. In contrast, glutathione had no significant effect on ABCC10 ATPase activity at approximately 1 μmol/L, a concentration stimulatory for ABCC1 (Fig. 3D). As controls, we confirmed that leukotriene C4 and glutathione are ATPase-inducing substrates for ABCC1 (Fig. 3E and F; refs. 9, 20, 21). Taken together, these data indicate that while LTC_4 and $E_2$17βG interact similarly with the ABCC1 and ABCC10 ATPase domains, glutathione does not stimulate ABCC10 ATPase activity. We observed that at high concentrations all substrates inhibited ABCC1 and ABCC10 ATPase activity as previously described for ABCB1 (33). It has been previously described that ABC transporter substrates can be categorized into 3 distinct types: (i) agents that stimulate ATPase activity at low concentration but inhibit activity at high concentration; (ii) agents that enhance ATPase activity in a dose-dependent manner; and (iii) agents that inhibit ATPase activity (as for ABCB1; ref. 34). Therefore, the ABCC10 substrates LTC_4, and $E_2$17βG are classified into the first group and glutathione falls into the third class of agents.

We have shown that the growth of ABCC10-transfected HEK293 cells is resistant to taxanes, vinca alkaloids, the non-taxane antimicrotubule agent epothilone, and the nucleoside analog Ara-C, but not to cisplatin (7, 35). We assessed the drug-stimulatable ATPase activity of ABCC10 using 2 drug concentrations (0.625 and 5 μmol/L) of the taxanes (docetaxel and paclitaxel), Ara-C, epothilone B, and cisplatin. We used vector transfected pFastBac membranes as a control, and ABCB1-overexpressing membranes for comparison (Fig. 4A–C). A maximal 31.8% stimulation in activity of ABCC10 was induced by Ara-C at a concentration of 0.625 μmol/L and (Fig. 4A). At 5 μmol/L, paclitaxel, and docetaxel stimulated ABCC10 ATPase activity by 15% and 24.38%, respectively (Fig. 4B), whereas in contrast, these compounds stimulated ABCB1 ATPase activity by 63% and 36%, respectively. However, the basal ATPase activity for ABCB1 was reduced 3-fold in comparison with

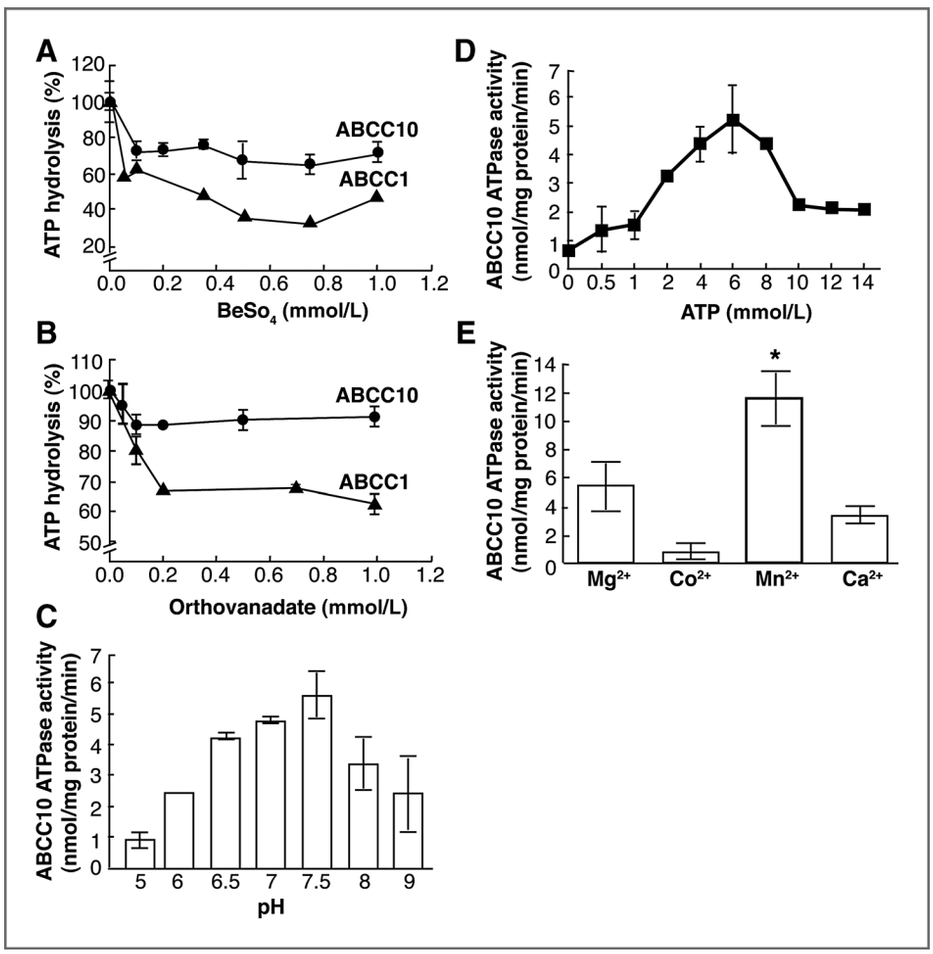

Figure 2. ABCC10- and ABCC1-mediated hydrolysis. For all experiments, data are mean ± SD of triplicate determinations. Graphs represent combined data from 3 separate experiments of ABCC10 (closed circles) or ABCC1, (closed triangles). A and B, steady state ATP hydrolysis was measured in ABCC10- and ABCC1-containing crude membranes in the presence of increasing concentrations of BeFx (A) or Vi (B). C, ABCC10 ATPase activity at various pHs. D, BeFx-sensitive ABCC10 ATPase activity was measured at several ATP concentrations (2, 5, 8, 10, 12, and 14 mmol/L). E, ABCC10 ATPase activity of membrane protein (10 μg) was assayed with 2× assay buffer containing 10 mmol/L $MnCl_2$, $MgCl_2$, $CaCl_2$, or $CoCl_2$. *, significant increase in ABCC10 ATPase activity ($P = 0.0178$) compared with Mg^{2+}.

ABCC10 activity. (Fig. 4C). Surprisingly, epothilone B did not affect ABCC10 ATPase activity, even though overexpressed ABCC10 causes resistance to this compound (7). As expected, the negative control cisplatin, a nonsubstrate (6), did not influence the ATPase activity ATPase activity of ABCC10 or ABCC1.

Localization and docetaxel transport properties of ABCC10 in polarized LLC-PK1 cells

ABC transporters variously localize to the apical or basolateral cell surface, affecting their transport properties (36, 37). To study the localization and transport properties of ABCC10, we overexpressed ABCC10 in a polarized pig kidney epithelial cell line, LLC-PK1 (Fig. 5A). ABCC10 localized predominantly to the basolateral membranes in 2 independent ABCC10-overexpressing LLC-PK1 derivative cell lines (Fig. 5B).

As anticipated, these ABCC10-overexpressing cell lines exhibited reduced accumulation of [^{3}H]-docetaxel compared with parental vector-transfected LLC-pcDNA3.1 cells (51% and 63%, respectively, at 60 minutes time point; Fig. 6A). A transepithelial well assay was used to assess transport of [^{3}H]-docetaxel initially added to either the apical or the basolateral side of a cell monolayer. Polarized LLC-PK1 ABCC10-overexpressing cells line predominantly exported [^{3}H]-docetaxel from the apical to the basolateral side (Fig. 6B). While the parental cell line revealed no differences between apical-to-basolateral or basolateral-to-apical docetaxel transport, in contrast, we found that apical-to-basolateral transport of ABCC10-overexpressing derivative cell lines were 70% to 80% higher than for LLC-PK1 parental apical-to-basolateral transport. These data correlated with the localization of ABCC10 (Fig. 5); ABCC10's basolateral localization indicated that ABCC10-dependent transport should be directional from the apical-to-basolateral side.

Cepharanthine and TKIs modulate ABCC10 ATPase activity, accumulation, and transcellular transport of [^{3}H]-docetaxel

The natural product cepharanthine has previously been established as a modulator of ABCC10-dependent resistance and transport activity (38). Clinically valuable TKIs, such as imatinib, lapatinib, erlotinib, and nilotinib, have also been shown to inhibit ABCC10 *in vitro* (39–41). We determined that at 5 μmol/L, cepharanthine, sorafenib, imatinib, nilotinib, erlotinib, and lapatinib were effective inhibitors of ABCC10 ATPase activity. At 0.625 μmol/L, nilotinib and erlotinib potently inhibited ABCC10 ATPase activity by 41.4% and

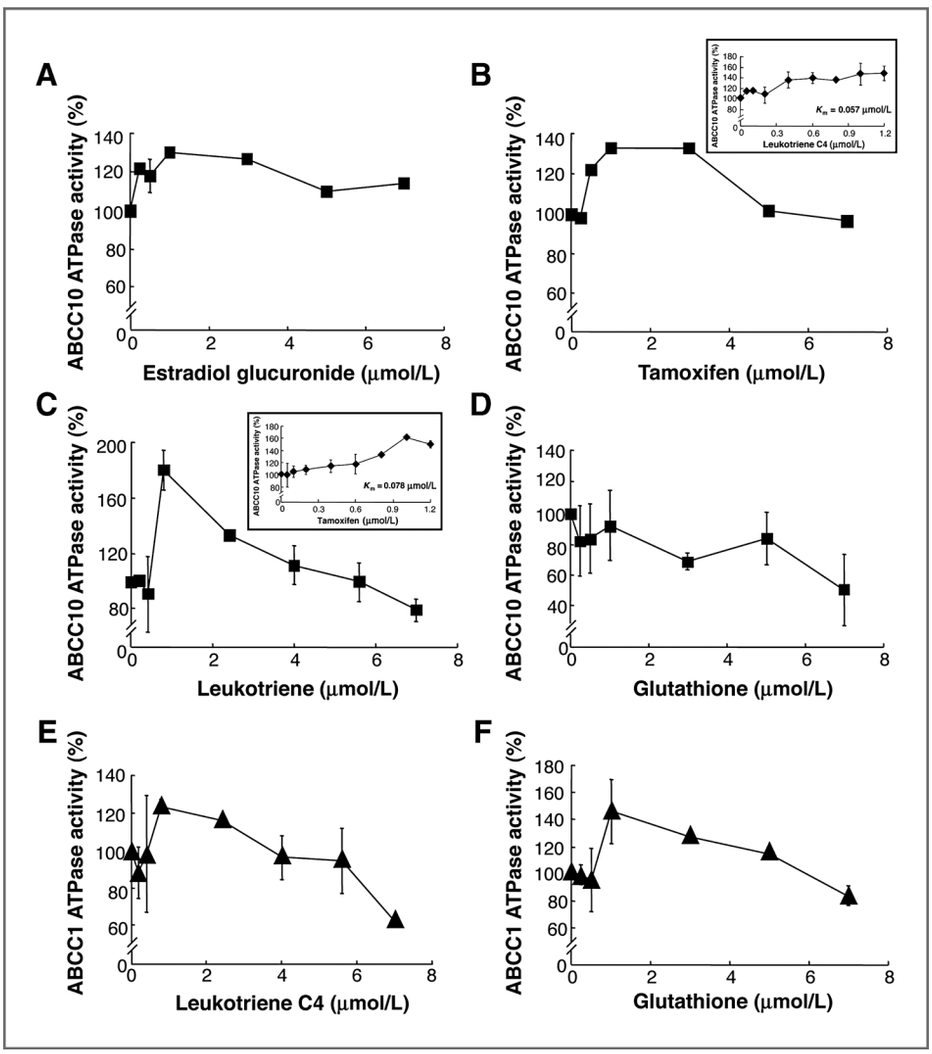

Figure 3. Effect of LTC_4, glutathione, E217βG, and tamoxifen on ABCC10 ATPase activity. Effect of $E_2$17βG (A), tamoxifen (B), LTC_4 (C), or glutathione (D) on ABCC10 ATPase activity. Effect of LTC_4 (E) or glutathione (F) on ABCC1 ATPase activity. Data points are mean ± SD of triplicate determination. Graphs represent combined data from 3 separate experiments of ABCC10 (closed circles) or ABCC1 (closed triangles).

47%, respectively (Fig. 7A). Finally, dasatinib had no effect on ATPase activity of ABCC10 at any concentration tested.

Treatment of ABCC10-overexpressing cells (LLC-ABCC10-11 and LLC-ABCC10-16) with 5 μmol/L cepharanthine significantly increased accumulation of [^{3}H]-docetaxel (by 48.4% and 22.5%, at 60 minutes, respectively), compared with accumulation levels without inhibitor. In contrast, 2.5 μmol/L sorafenib increased [^{3}H]-docetaxel accumulation by 22.4% in LLC-ABCC10-16 cells and by 49% in LLC-ABCC10-11 cells, compared with accumulation levels without inhibitor (Fig. 7B). A total of 2.5 μmol/L dasatinib also increased [^{3}H]-docetaxel intracellular accumulation without significant effects on ABCC10 ATPase activity. Conversely, 2.5 μmol/L lapatinib (a reported ABCC10 reversal agent (40) did not affect the accumulation levels of docetaxel but decreased ABCC10 ATPase activity. Other TKIs with reported activity in inhibiting ABCC10, such as nilotinib and erlotinib, only affected [^{3}H]-docetaxel accumulation of the LLC-ABCC10-11 cell line, whereas imatinib only inhibited the LLC-ABCC10-16 cell line (Fig. 7B). Interestingly, nilotinib, dasatinib, imatinib, and lapatinib significantly decreased [^{3}H]-docetaxel accumulation of the parental LLC-pcDNA3.1 cell line, indicating additional activities not targeted at ABCC10.

Because our data revealed that [^{3}H]-docetaxel accumulation was significantly inhibited by sorafenib in both transfectants, we tested if sorafenib could also inhibit ABCC10-transepithelial transport using cepharanthine as a positive control. We showed that cepharanthine was the most potent inhibitor of ABCC10-mediated [^{3}H]-docetaxel accumulation in both transfectants (Fig. 7B). Finally, we also established that transepithelial apical-to-basolateral transport of labeled docetaxel was inhibited by 5 μmol/L cepharanthine in LLC-ABCC10-16 (Fig. 7C). A total of 2.5 μmol/L sorafenib maximally inhibited apical-to-basolateral transport for the LLC-ABCC10-16 cell line at 6 to 30 minutes (Fig. 7C).

Discussion

To date, the localization, biochemical, and transport properties of ABCC10 have been largely unexplored, with the exception of a single study that used a membrane vesicle

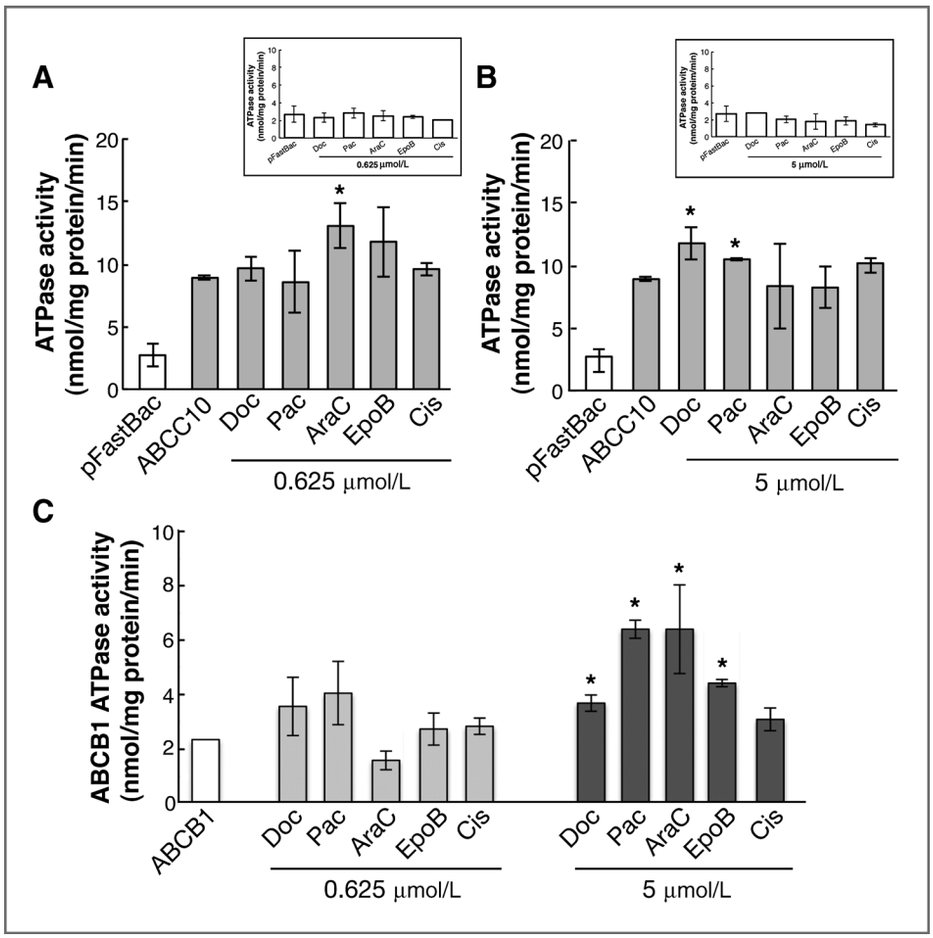

Figure 4. Stimulation of ABCC10 activity by anticancer drugs. Survey of ABCC10 (A and B) and pFastBac-control (4A inset and 4B inset), ABCB1 (C) ATPase activity was conducted after addition of 2 separate concentrations of docetaxel (Doc), paclitaxel (Pac), epothilone B (EpoB), cytarabine (Ara-C), and cisplatin (Cis). A and B, 0.625 μmol/L (A) and 5 μmol/L (B). Bars represent the mean of 3 separate experiments carried out in duplicate ± SD. Statistical analysis was calculated using a Student unpaired *t* test; *P* values for ABCC10 are 0.0288 (docetaxel), 0.0169 (paclitaxel), and 0.0124 (cytarabine); *P* values for ABCB1 are 0.0456 (docetaxel), 0.0168 (paclitaxel), 0.0319 (cytarabine), and 0.0495 (epothilone B). *, $P < 0.05$.

transport system (42). In the present study, the biochemical properties of ABCC10 were compared with the well-described properties of ABCC1, the first identified ABCC subfamily member (20). Despite significant sequence identity (50.3%/52.7%) within the 2 NBDs and appreciable overall amino acid identity (33.8%) between ABCC10 and ABCC1 (6), ABCC10 transports taxanes and confers *in vivo* taxane resistance and does not require glutathione for transport, in contrast to

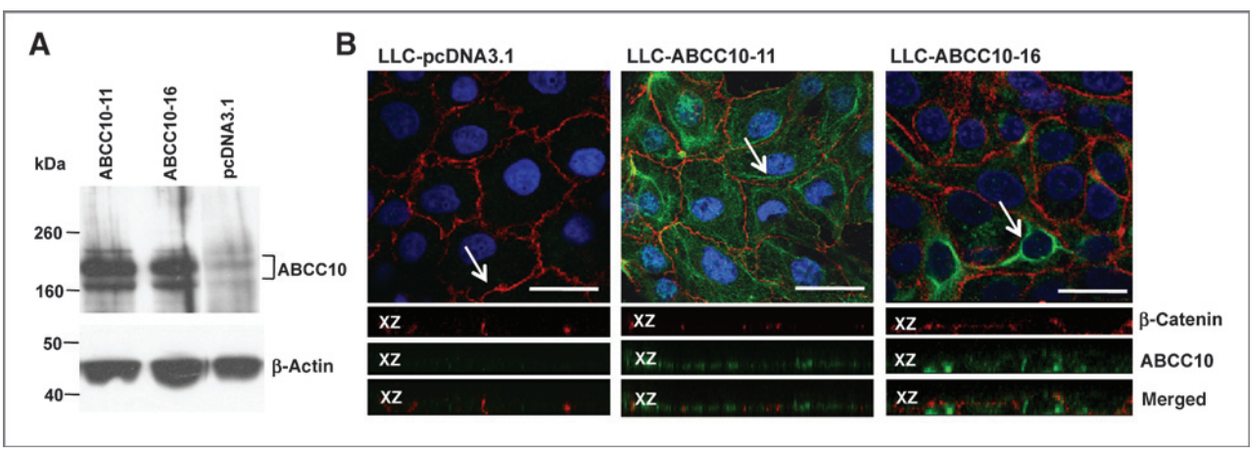

Figure 5. Detection of expression by Western blot analysis and localization of ABCC10 in LLC-ABCC10 monolayers. A, 30 μg of crude membranes prepared from LLC-PK1, LLC-ABCC10-11, and LLC-ABCC10-16 cells was analyzed by Western blot analysis. The ABCC10 monoclonal antibody detected 2 bands with apparent M_r approximately 168,000 kDa and 202,000 kDa. B, immunofluorescence analysis of confluent LLC-PK1 cells transfected with pcDNA 3.1 (left) and LLC-PK1 cells transfected with ABCC10 expression vector (middle and right). ABCC10 (green), β-catenin (red), and DAPI-stained DNA (blue) are indicated. Arrows indicate the location of *xz*-section shown later each panel. Scale bar, 20 μmol/L, ×60 magnification.

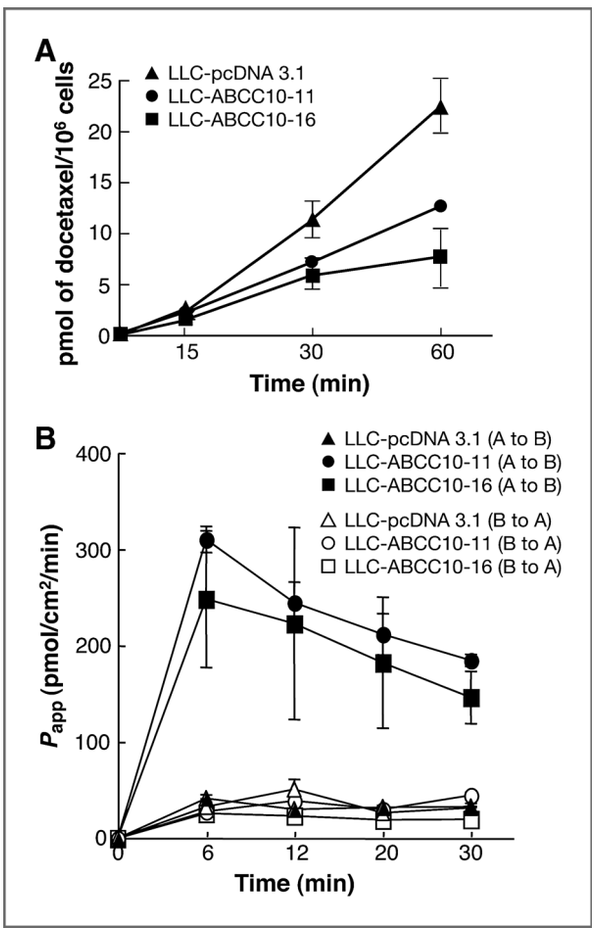

Figure 6. Accumulation and transepithelial transport of [^{3}H]-docetaxel. A, cellular accumulation of [^{3}H]-docetaxel in LLC-PK–transfected cell lines compared with parental cells. B, basolateral to apical or apical-to-basolateral transport of [^{3}H]-docetaxel. At 6 minutes, the P values = 0.0063 for LLC-ABCC10-16 and 0.0202 for LLC-ABCC10-11. Representative data are shown for LLC-ABCC10-11 (circles), LLC-ABCC10-16 (squares) transfectant lines, and the LLC-pcDNA3.1 control line (triangles); full symbols indicate apical-to-basolateral (A to B) transport and empty symbols indicate basolateral to apical (B to A) transport.

ABCC1 (6). Our characterization of ABCC10 basal activity revealed that ABCC10 was far less sensitive to vanadate (11%) or BeFx (32%) inhibition than ABCC1 (35% and 60%, respectively), or the other major taxane pump, ABCB1, which has been reported to be completely inhibited (43). Taken together, these data imply that the catalytic cycle of ABCC10 differs from the well-described cycles of ABCC1 and ABCB1. As anticipated, we found that ABCC10 ATPase activity is stimulated by its substrates, the taxanes and Ara-C, similar to the best-described taxane pump, ABCB1 (44). Surprisingly, however, the extremely weak ABCC10 transport substrate LTC_4, stimulated ABCC10 activity significantly more than ABCC1 activity (~80% vs. ~30%), even though LTC_4 is a well-established physiologic substrate for ABCC1. This unexpected result further highlights differences between these proteins, and emphasizes the need for further study (9, 45).

Knowledge of intracellular distribution is important for understanding the potential effects of ABCC10-mediated transport in normal tissues, and to provide insight with respect to putative substrates. In the present study, we have shown that ABCC10 localizes basolaterally when ectopically expressed in the LLC-PK1 kidney cell line, similar to the localization reported for ABCC1 in small intestine and kidney cells. In contrast, ABCB1 localizes apically in brain, liver, small intestine, and kidney (46, 47). ABCC10 transcript expression is widespread, with highest levels detected in the gonads and spleen (7). The ABCC10 transcript has been detected in multiple types of adenocarcinoma that are routinely treated with taxanes, including breast, ovary, and lung (4, 48). Recent studies have shown that ABCC10 is also upregulated in hepatocellular carcinoma compared with normal adjacent healthy liver samples (49), and that ABCC10 gene levels in colorectal tumors correlate with tumor grade ($P = 0.01$; ref. 50), implying that increased ABCC10 expression might be a biomarker for and regulator of treatment response in certain cancers. However, besides a single study examining ABCC10 protein expression in lung cancer (5), no studies have been published about ABCC10 protein expression. It will be of considerable interest to assess ABCC10 protein expression levels in tumors versus normal tissues in the context of treatment with taxanes.

Our recent work has indicated that loss of Abcc10 function *in vivo* causes taxane sensitization (15). In this report, we have shown that cepharanthine and sorafenib (an agent used to treat unresectable and advanced hepatocellular carcinoma) were effective inhibitors of ABCC10 ATPase activity. Likewise, we showed that cepharanthine increased docetaxel accumulation in ABCC10-overexpressing cells and inhibited apical-to-basolateral transport, particularly at early timepoints (at 6–12 minutes). Interestingly, we found that sorafenib promoted increased [H^3]-docetaxel accumulation in 2 LLC-ABCC10 transfectants. The identification of sorafenib as an ABCC10 inhibitor suggests that *in vivo* action of this inhibitor may involve modulation of ABCC10-dependent docetaxel transport. Currently, no identified inhibitors have been shown to have *in vivo* efficacy against ABCC10; an important goal for future work would be the exploration of the ability of sorafenib, cepharanthine, and other putative inhibitors to modulate *in vivo* taxane transport capabilities of ABCC10 in preclinical models. ABCC10 inhibition is particularly nominated as a potentially high value target for inhibition based on its physiologic relevance to *in vivo* taxane resistance. The loss of no other single transporter (including ABCB1) has resulted in tissue sensitization to taxanes, suggesting no other transporter can be upregulated to compensate for Abcc10 loss (15). Whether absence of ABCC10 sensitizes solid tumors to taxanes while not leading to unacceptable toxicity in normal tissue remains to be determined. These investigations are currently ongoing in our laboratory.

In summary, this study provided the first analysis of ABCC10 ATPase activity, showed that ABCC10 localized basolaterally in a polarized kidney cell line, and confirmed this localization by showing apical-to-basolateral transport. Importantly, we also

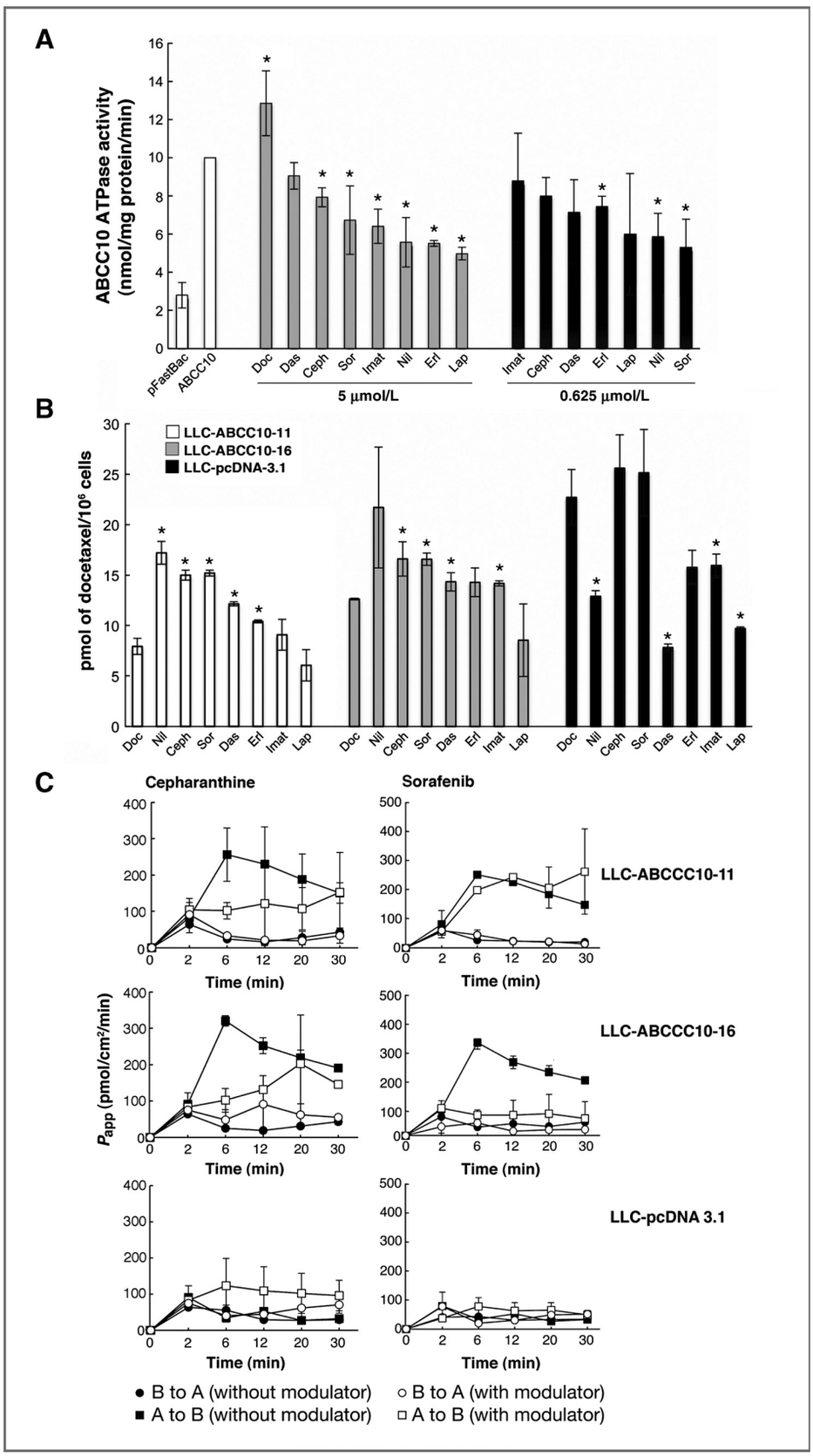

Figure 7. Effect of modulators on ABCC10 ATPase activity and accumulation of [^{3}H]-docetaxel. For all experiments, each point represents the mean ± SD of 3 experiments. A, ATPase activity of ABCC10 in the presence of 5 or 0.625 μmol/L cepharanthine (Ceph) or sorafenib (Sor), dasatinib (Das), imatinib (Imat), nilotinib (Nil), erlotinib (Erl), lapatinib (Lap); 2.5 μmol/L. *P* values at 5 μmol/L are 0.0219 (cepharanthine), 0.0434 (sorafenib), 0.024 (imatinib), 0.0431 (nilotinib), 0.002 (erlotinib), and 0.012 (lapatinib). *P* values at 0.625 μmol/L are 0.0367 (erlotinib) and 0.0333 (nilotinib). B, cellular accumulation of [^{3}H]-docetaxel in cells treated with cepharanthine or TKIs. *P* value in LLC-ABCC10-11 and LLC-ABCC16, respectively: for cepharanthine = 0.0472, 0.0218; for sorafenib = 0.0491, 0.0046; for dasatinib = 0.0155, 0.0265; for erlotinib in LLC-ABCC10-11 = 0.0423; for nilotinib in LLC-ABCC10-11 = 0.0104; and for imatinib in LLC-ABCC10-16 = 0.0062. C, effect of modulators on the basolateral-to-apical or apical-to-basolateral transport of [^{3}H]-docetaxel. Basolateral-to-apical, and apical-to-basolateral transport of [^{3}H]-docetaxel in cells treated with cepharanthine or sorafenib. For 5 μmol/L cepharanthine treatment of LLC-ABCC10-16 and LLC-ABCC10-11, $P = 0.0312$ and $P = 0.05$ at 6 minutes, respectively. For 2.5 μmol/L sorafenib, the LLC-ABCC10-16 cell line showed maximal inhibition of apical-to-basolateral transport at 6 minutes ($P = 0.0341$). *, $P < 0.05$. For all experiments, each point represents the mean ± SD of 3 experiments. Curves shown represent apical-to-basolateral transport (squares); basolateral-to-apical transport (circles); without modulator (full symbols); and with modulator (open symbols).

identified a novel inhibitor of ABCC10 transport. These ABCC10 assays can be used to identify and validate potential ABCC10 modulators that can be validated in preclinical models with the goal to increase the clinical effectiveness of ABCC10 drug substrates.

Disclosure of Potential Conflicts of Interest

No potential conflicts of interest were disclosed.

Authors' Contributions

Conception and design: E.A. Hopper-Borge
Development of methodology: E.V. Malofeeva, M. Gudima, E.A. Hopper-Borge
Acquisition of data (provided animals, acquired and managed patients, provided facilities, etc.): E.V. Malofeeva, M. Gudima, E.A. Hopper-Borge
Analysis and interpretation of data (e.g., statistical analysis, biostatistics, computational analysis): N. Domanitskaya, M. Gudima, E.A. Hopper-Borge
Writing, review, and/or revision of the manuscript: E.V. Malofeeva, M. Gudima, E.A. Hopper-Borge
Administrative, technical, or material support (i.e., reporting or organizing data, constructing databases): M. Gudima, E.A. Hopper-Borge
Study supervision: E.A. Hopper-Borge
Conducted localization experiments: N. Domanitskaya

Acknowledgments

The authors thank Drs. Suresh Ambudkar (National Cancer Institute) for his guidance, advice, and help in preparation of the initial ABCC10 virus used in this project; Michael Gottesman for the ABCB1 (MDR1) cDNA; Susan Cole for the MRP1 cDNA; Jonathan Chernoff and Jeffrey R. Peterson (Fox Chase Cancer Center) for helpful discussions and review of the article; and Erica A. Golemis (Fox Chase Cancer Center) for critical reading and review of the article. The authors also thank Karen Trush for assistance with preparation of the figures.

Grant Support

This work was supported by NIH grants K01CA120091 to E.A. Hopper-Borge, and CA06927 to Fox Chase Cancer Center.

The costs of publication of this article were defrayed in part by the payment of page charges. This article must therefore be hereby marked *advertisement* in accordance with 18 U.S.C. Section 1734 solely to indicate this fact.

Received April 6, 2012; revised August 24, 2012; accepted October 1, 2012; published OnlineFirst October 19, 2012.

References

1. Keppler D. Multidrug resistance proteins (MRPs, ABCCs): importance for pathophysiology and drug therapy. Handb Exp Pharmacol 2011:299–323.
2. Glavinas H, Krajcsi P, Cserepes J, Sarkadi B. The role of ABC transporters in drug resistance, metabolism and toxicity. Curr Drug Deliv 2004;1:27–42.
3. Kruh GD, Guo Y, Hopper-Borge E, Belinsky MG, Chen ZS. ABCC10, ABCC11, and ABCC12. Pflugers Arch 2007;453:675–84.
4. Takayanagi S, Kataoka T, Ohara O, Oishi M, Kuo MT, Ishikawa T. Human ATP-binding cassette transporter ABCC10: expression profile and p53-dependent upregulation. J Exp Ther Oncol 2004; 4:239–46.
5. Wang P, Zhang Z, Gao K, Deng Y, Zhao J, Liu B, et al. Expression and clinical significance of ABCC10 in the patients with non–small cell lung cancer. Zhongguo Fei Ai Za Zhi 2009;12:875–8.
6. Hopper-Borge E, Chen ZS, Shchaveleva I, Belinsky MG, Kruh GD. Analysis of the drug resistance profile of multidrug resistance protein 7 (ABCC10): resistance to docetaxel. Cancer Res 2004;64:4927–30.
7. Hopper-Borge E, Xu X, Shen T, Shi Z, Chen ZS, Kruh GD. Human multidrug resistance protein 7 (ABCC10) is a resistance factor for nucleoside analogues and epothilone B. Cancer Res 2009;69:178–84.
8. Oguri T, Ozasa H, Uemura T, Bessho Y, Miyazaki M, Maeno K, et al. MRP7/ABCC10 expression is a predictive biomarker for the resistance to paclitaxel in non–small cell lung cancer. Mol Cancer Ther 2008;7:1150–5.
9. Mao Q, Leslie EM, Deeley RG, Cole SP. ATPase activity of purified and reconstituted multidrug resistance protein MRP1 from drug-selected H69AR cells. Biochim Biophys Acta 1999;1461:69–82.
10. Hagmann W, Nies AT, Konig J, Frey M, Zentgraf H, Keppler D. Purification of the human apical conjugate export pump MRP2 reconstitution and functional characterization as substrate-stimulated ATPase. Eur J Biochem 1999;265:281–9.
11. Chloupkova M, Pickert A, Lee JY, Souza S, Trinh YT, Connelly SM, et al. Expression of 25 human ABC transporters in the yeast *Pichia pastoris* and characterization of the purified ABCC3 ATPase activity. Biochemistry 2007;46:7992–8003.
12. Cai J, Daoud R, Alqawi O, Georges E, Pelletier J, Gros P. Nucleotide binding and nucleotide hydrolysis properties of the ABC transporter MRP6 (ABCC6). Biochemistry 2002;41:8058–67.
13. Sauna ZE, Nandigama K, Ambudkar SV. Multidrug resistance protein 4 (ABCC4)-mediated ATP hydrolysis: effect of transport substrates and characterization of the post-hydrolysis transition state. J Biol Chem 2004;279:48855–64.
14. Sauna ZE, Smith MM, Muller M, Kerr KM, Ambudkar SV. The mechanism of action of multidrug-resistance-linked P-glycoprotein. J Bioenerg Biomembr 2001;33:481–91.
15. Hopper-Borge EA, Churchill T, Paulose C, Nicolas E, Jacobs JD, Ngo O, et al. Contribution of Abcc10 (Mrp7) to *in vivo* paclitaxel resistance as assessed in Abcc10(−/−) mice. Cancer Res 2011;71:3649–57.
16. Towbin H, Staehelin T, Gordon J. Electrophoretic transfer of proteins from polyacrylamide gels to nitrocellulose sheets: procedure and some applications. 1979. Biotechnology 1992;24:145–9.
17. DeGorter MK, Conseil G, Deeley RG, Campbell RL, Cole SP. Molecular modeling of the human multidrug resistance protein 1 (MRP1/ABCC1). Biochem Biophys Res Commun 2008;365:29–34.
18. Irvine JD, Takahashi L, Lockhart K, Cheong J, Tolan JW, Selick HE, et al. MDCK (Madin-Darby canine kidney) cells: a tool for membrane permeability screening. J Pharm Sci 1999;88:28–33.
19. Spears KJ, Ross J, Stenhouse A, Ward CJ, Goh LB, Wolf CR, et al. Directional trans-epithelial transport of organic anions in porcine LLC-PK1 cells that co-express human OATP1B1 (OATP-C) and MRP2. Biochem Pharmacol 2005;69:415–23.
20. Deeley RG, Cole SP. Substrate recognition and transport by multidrug resistance protein 1 (ABCC1). FEBS Lett 2006;580:1103–11.
21. Cole SP, Deeley RG. Transport of glutathione and glutathione conjugates by MRP1. Trends Pharmacol Sci 2006;27:438–46.
22. Lanzetta PA, Alvarez LJ, Reinach PS, Candia OA. An improved assay for nanomole amounts of inorganic phosphate. Anal Biochem 1979;100:95–7.
23. Sankaran B, Bhagat S, Senior AE. Inhibition of P-glycoprotein ATPase activity by beryllium fluoride. Biochemistry 1997;36:6847–53.
24. Rao US. Drug binding and nucleotide hydrolyzability are essential requirements in the vanadate-induced inhibition of the human P-glycoprotein ATPase. Biochemistry 1998;37:14981–8.
25. Hipfner DR, Deeley RG, Cole SP. Structural, mechanistic and clinical aspects of MRP1. Biochim Biophys Acta 1999;1461:359–76.
26. Kerr KM, Sauna ZE, Ambudkar SV. Correlation between steady-state ATP hydrolysis and vanadate-induced ADP trapping in human P-glycoprotein. Evidence for ADP release as the rate-limiting step in the catalytic cycle and its modulation by substrates. J Biol Chem 2001;276:8657–64.
27. Marchetti S, Oostendorp RL, Pluim D, van Eijndhoven M, van Tellingen O, Schinkel AH, et al. *In vitro* transport of gimatecan (7-t-butoxyiminomethylcamptothecin) by breast cancer resistance protein, P-glycoprotein, and multidrug resistance protein 2. Mol Cancer Ther 2007;6(12 Pt 1):3307–13.
28. Shibayama Y, Nakano K, Maeda H, Taguchi M, Ikeda R, Sugawara M, et al. Multidrug resistance protein 2 implicates anticancer drug-resistance to sorafenib. Biol Pharm Bull 2011;34:433–5.
29. Syroeshkin AV, Galkin MA, Sedlov AV, Vinogradov AD. Kinetic mechanism of Fo x F1 mitochondrial ATPase: Mg^{2+} requirement for Mg x ATP hydrolysis. Biochemistry (Mosc) 1999;64:1128–37.

30. Kerr ID. Structure and association of ATP-binding cassette transporter nucleotide-binding domains. Biochim Biophys Acta 2002;1561:47–64.
31. Hooijberg JH, Pinedo HM, Vrasdonk C, Priebe W, Lankelma J, Broxterman HJ. The effect of glutathione on the ATPase activity of MRP1 in its natural membranes. FEBS Lett 2000;469:47–51.
32. Mao Q, Deeley RG, Cole SP. Functional reconstitution of substrate transport by purified multidrug resistance protein MRP1 (ABCC1) in phospholipid vesicles. J Biol Chem 2000;275:34166–72.
33. Najar IA, Sachin BS, Sharma SC, Satti NK, Suri KA, Johri RK. Modulation of P-glycoprotein ATPase activity by some phytoconstituents. Phytother Res 2010;24:454–8.
34. Zhao XQ, Xie JD, Chen XG, Sim HM, Zhang X, Liang YJ, et al. Neratinib reverses ATP-binding cassette B1-mediated chemotherapeutic drug resistance *in vitro*, *in vivo*, and *ex vivo*. Mol Pharmacol 2012;82:47–58.
35. Hopper E, Belinsky MG, Zeng H, Tosolini A, Testa JR, Kruh GD. Analysis of the structure and expression pattern of MRP7 (ABCC10), a new member of the MRP subfamily. Cancer Lett 2001;162:181–91.
36. Evers R, Zaman GJ, van Deemter L, Jansen H, Calafat J, Oomen LC, et al. Basolateral localization and export activity of the human multidrug resistance-associated protein in polarized pig kidney cells. J Clin Invest 1996;97:1211–8.
37. Deeley RG, Westlake C, Cole SP. Transmembrane transport of endo- and xenobiotics by mammalian ATP-binding cassette multidrug resistance proteins. Physiol Rev 2006;86:849–99.
38. Zhou Y, Hopper-Borge E, Shen T, Huang XC, Shi Z, Kuang YH, et al. Cepharanthine is a potent reversal agent for MRP7(ABCC10)-mediated multidrug resistance. Biochem Pharmacol 2009;77:993–1001.
39. Hoffmann K, Franz C, Xiao Z, Mohr E, Serba S, Buchler MW, et al. Sorafenib modulates the gene expression of multi-drug resistance mediating ATP-binding cassette proteins in experimental hepatocellular carcinoma. Anticancer Res 2010;30:4503–8.
40. Kuang YH, Shen T, Chen X, Sodani K, Hopper-Borge E, Tiwari AK, et al. Lapatinib and erlotinib are potent reversal agents for MRP7 (ABCC10)-mediated multidrug resistance. Biochem Pharmacol 2010;79:154–61.
41. Shen T, Kuang YH, Ashby CR, Lei Y, Chen A, Zhou Y, et al. Imatinib and nilotinib reverse multidrug resistance in cancer cells by inhibiting the efflux activity of the MRP7 (ABCC10). PLoS ONE 2009;4:e7520.
42. Chen ZS, Hopper-Borge E, Belinsky MG, Shchaveleva I, Kotova E, Kruh GD. Characterization of the transport properties of human multidrug resistance protein 7 (MRP7, ABCC10). Mol Pharmacol 2003;63:351–8.
43. Urbatsch IL, Sankaran B, Weber J, Senior AE. P-glycoprotein is stably inhibited by vanadate-induced trapping of nucleotide at a single catalytic site. J Biol Chem 1995;270:19383–90.
44. Brooks TA, Minderman H, O'Loughlin KL, Pera P, Ojima I, Baer MR, et al. Taxane-based reversal agents modulate drug resistance mediated by P-glycoprotein, multidrug resistance protein, and breast cancer resistance protein. Mol Cancer Ther 2003;2:1195–205.
45. Robbiani DF, Finch RA, Jager D, Muller WA, Sartorelli AC, Randolph GJ. The leukotriene C(4) transporter MRP1 regulates CCL19 (MIP-3beta, ELC)-dependent mobilization of dendritic cells to lymph nodes. Cell 2000;103:757–68.
46. Sarkadi B, Homolya L, Szakacs G, Varadi A. Human multidrug resistance ABCB and ABCG transporters: participation in a chemoimmunity defense system. Physiol Rev 2006;86:1179–236.
47. Kruh GD, Belinsky MG. The MRP family of drug efflux pumps. Oncogene 2003;22:7537–52.
48. Dabrowska M, Sirotnak F. Regulation of transcription of the human MRP7 gene. Characteristics of the basal promoter and identification of tumor-derived transcripts encoding additional 5′ end heterogeneity. Gene 2004;341:129–39.
49. Borel F, Han R, Visser A, Petry H, van Deventer SJ, Jansen PL, et al. Adenosine triphosphate-binding cassette transporter genes up-regulation in untreated hepatocellular carcinoma is mediated by cellular microRNAs. Hepatology 2012;55:821–32.
50. Hlavata I, Mohelnikova-Duchonova B, Vaclavikova R, Liska V, Pitule P, Novak P, et al. The role of ABC transporters in progression and clinical outcome of colorectal cancer. Mutagenesis 2012;27:187–96.